공학석사학위논문

인체 보행특성을 고려한 전방향 에너지 하베스팅 보도블록의 신뢰성 기반 최적설계

Reliability-Based Design Optimization of Omnidirectional Energy Harvesting Sidewalk Block Considering Human Gait Analysis

2015 년 8 월

서울대학교 대학원

기계항공공학부

CUI JINSHI

Abstract

Reliability-Based Design Optimization of Omnidirectional Energy Harvesting Sidewalk Block Considering Human Gait Analysis

CUI JINSHI
Department of Mechanical and Aerospace Engineering
The Graduate School
Seoul National University

Piezoelectric energy harvesting (PEH) which scavenges electric power from ambient, otherwise wasted, mechanical energy has received significant attention as an ultimate solution to possibly eliminate batteries for powering portable electronics. As a compact and durable design paradigm of a piezoelectric energy harvester, energy harvesting skin (EH skin) which can be directly attached onto the surface of an engineered system has been proposed and thus requires no need for clamping fixtures and proof mass. The objective of this thesis is to propose an innovative energy harvesting sidewalk block concept by advancing the design methodology of EH skin. Even though few energy harvesting sidewalk blocks have been commercialized, however, there has been no scientific approach to design an energy harvesting sidewalk block considering human gait analysis. This thesis thus presents a systematic design methodology for the omnidirectional energy harvesting (OEH) sidewalk block considering human gait, which consists of four sequentially-executed tasks as: 1) the extraction of a loading profile from ground reaction force of normal gait, 2) the multiphysics modeling with finite element method (FEM) to estimate the time-variant stress and output voltage of OEH sidewalk block according to gait cycle, 3) development of conceptual design of OEH sidewalk block, and 4) reliability-based design optimization (RBDO) of OEH sidewalk block. In RBDO, the design problem is formulated as the maximization of the output energy subjected to fatigue failure constraints in a probabilistic manner. Since Kriging and polynomial surrogate models are constructed based on the Latin Hypercube sampling (LHS) for design of experiment (DOE). Monte Carlo Simulation (MCS) was used to calculate the reliability for a probabilistic constraint with affordable computational effort. To the best of the author's knowledge, this study is the pioneering work to perform RBDO of OEH sidewalk block while accounting directional uncertainty in human gait as well as variability in material properties and geometry.

Keywords: Piezoelectric Energy Harvesting
Omnidirectional Energy Harvesting Sidewalk Block
Human Gait Analysis
Voltage Cancellation
Multiphysics Electromechanical Simulation
Reliability-Based Design Optimization
Surrogate Model

Student Number: 2013-23827

Table of Contents

List of Tables

List of Figures

Nomenclatures

α	direction of footstep
τ	time constant
R	external resistance
C	capacitance
$\bar{\varepsilon}_{33}^{S}$	relative permittivity at constant strain
A	area of piezoelectric patch
h_p	thickness of the piezoelectric patch
E	electrical energy
$\mathbf{d}$	design vector
nd	number of design variables
$\mathbf{d}_\mathbf{L}$	lower bounds of design variables
$\mathbf{d}_\mathbf{U}$	upper bounds of design variables
$G(\mathbf{d})$	performance constraint
σ_{PZT}	maximum principal stress of piezoelectric patch
σ_e	fatigue strength of piezoelectric patch
nr	number of random variables
$\mathbf{X}$	random vector
R_t	target reliability

r_i	inner radius of doughnut shape
r_o	outer radius of doughnut shape
t	thickness of substrate
Y_s	Young' modulus of substrate
e_{31}	piezoelectric constant
c_{11}	elastic modulus
$\mu_i^{\mathrm{d,L}}$	lower mean value of design variable
$\mu_i^{\mathrm{d,U}}$	upper mean value of design variable
μ_i	mean value of noise variable
σ_i	standard deviation
i	number of design and noise variables
$\tilde{x}_i$	normalized value
x_i	physical value
$x_{i,\min}$	minimum physical value
$x_{i,\max}$	maximum physical value
β_o, β_{ii}, β_{ij}	coefficients of polynomial
x_i, x_j	design and noise variables
$f_j(x)$	fixed function
σ^2	process variance
$R^{'}$	correlation

a_i	coefficient
$\lVert \mathbf{X} - \mathbf{X}_{0i} \rVert$	Euclidean distance
$\hat{y}_i$	true value
$\bar{y}$	mean of true value
y_i	surrogate model
m	number of testing points

Chapter 1. Introduction

1.1 Motivation

With the development of IoT (Internet of Things), wireless sensor networks (WSNs) has received significant attention. Since WSNs is used to monitor space, objects, human beings, and interact among them, which is expected to be an important part to construct IoT. However, the limited life expectancy and high replacement cost of batteries havelf been most lagging parts to develop a self-powered wireless sensor networks [1]. Energy harvesting (EH), which is a technology that scavenges electric energy from ambient energy sources, has the potential to reduce batteries dependency and power the small-scale and, low-power electronic devices

Among the several existing EH technologies, piezoelectric energy harvesting (PEH) is one of the practical solutions to establish self- powered WSNs. PEH is that when piezoelectricity is mechanical strained, it can produce corresponding amount of electrical energy. Therefore, tremendous efforts have been made to convert mechanical energy into electrical energy using PEH including materials science, design, circuit configuration, and so on.

An energy harvesting sidewalk block is one of potential applications using piezoelectric transduction. Compared with a prevalent commonly used sidewalk block, energy harvesting sidewalk block which employs piezoelectric effect or electromagnetic effect generates electrical energy when people step on the sidewalk block. The generated electric energy can be used for charging rechargeable batteries for low-power traffic system or street lighting.

Even though extensive research efforts have been made to advance piezoelectric energy harvesting technology in a variety of fields as: (a) piezoelectric materials, (b) modeling and analysis, (c) mechanics-based design, (d) circuit configuration, and (e) system integration, however, commercially available energy harvesting sidewalk blocks have not been developed by a scientific approach. This fact means that systematic design rationales for energy harvesting sidewalk block have not been proposed yet. Furthermore, the physical interactions between the nature of human gait and the piezoelectric performance should be taken into account under a design process of energy harvesting sidewalk block. To successfully realize an effective and reliable energy harvesting sidewalk block, therefore, it is necessary to thoroughly understand its core technologies such as rigorous modeling, analysis, and design methodology.

To achieve this objective, three key research challenges should be carefully addressed: (1) how to consider scientific design rationales, (2) how to analyze the time-variant electromechanical behaviors under human gait cycle, and (3) how to reliably scavenge the output energy while accounting for the variability in geometry and material properties of energy harvesting sidewalk block.

1.2 Scope of Research

The scope of this thesis is to develop the following research thrust to address the above challenges:

Research thrust 1: Design rationales are presented from different points of view. The initial design of energy harvesting sidewalk block is considered from the following three aspects. First, human gait analysis is researched with respect to normal gait for an average male, and the load profile is extracted to apply transient force for analyzing energy harvesting sidewalk block. Second, this study assumes that people walk on the center of the sidewalk block, and the directional uncertainty of human gait on the center of a sidewalk block is considered when defining the position and shape of piezoelectric patch, but the positional uncertainty of human gait is out of the scope of this study. Third, since energy harvesting sidewalk block is developed based on the concept of fully clamped energy harvesting skin (EH skin) which is designed by directly attaching piezoelectric patch onto the engineering system, voltage cancellation effect is avoided by the piezoelectric segmentation method in this study to harvest more energy. Finally, the fatigue failure of omnidirectional energy harvesting (OEH) sidewalk block is considered as an important design constraint to obtain a reliability-based optimal design.

Research thrust 2: Time-variant mechanical stress and output voltage are calculated by multiphysics simulation. A normal gait is simulated in transient analysis by applying a ground reaction force as a loading condition. In addition, the relationship of the output voltage generated by OEH sidewalk block and energy dissipation due to time constant by an external electrical resistance are described using equivalent circuit model of piezoelectric transduction.

Research thrust 3: To ensure the reliability of OEH sidewalk block under physical uncertainty, reliability-based design optimization with a surrogate model is performed while accounting for uncertainties in gait cycle loading, geometry, and material properties.

The overall procedure of OEH sidewalk block development is summarized in Figure 1-1.

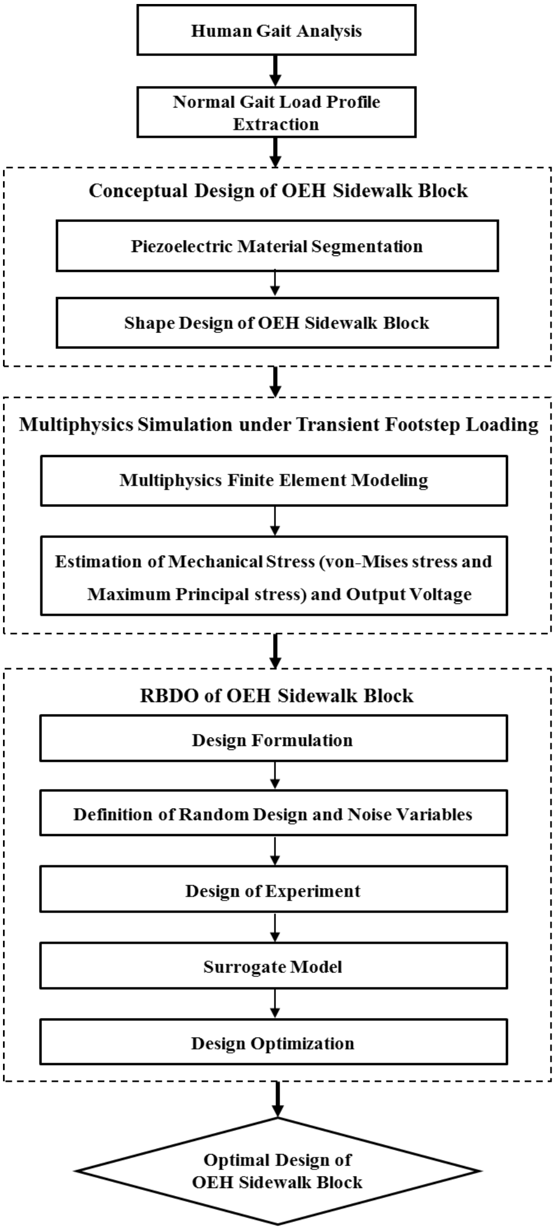

Figure 1-1 Framework of OEH Sidewalk Block Development

1.3 Thesis Layout

This thesis consists of seven chapters, which is organized as follows: Chapter 2 provides a brief review of PEH and the application - energy harvesting sidewalk block. Chapter 3 depicts human gait analysis which includes gait cycle and ground reaction force with respect to normal gait. Chapter 4 proposes the conceptual design of OEH sidewalk block based on the transient loading. Chapter 5 describes the process of multiphysics simulation under transient footstep loading. The reliability-based design optimization of OEH sidewalk block with a surrogate model is described in Chapter 6. Finally, Chapter 7 summarizes the contributions of this research and offers insightful discussion about future works.

Chapter 2. Literature Review

In this chapter, literature review on piezoelectric energy harvesting technology is provided with respect to energy harvesting sidewalk block. In Section 2.1, the fundamental theory of piezoelectricity, and the state-of-art research on methodology of a piezoelectric energy harvester are given. Furthermore, piezoelectric energy harvesting from human activities are reviewed briefly in Section 2.2

2.1 Review of Piezoelectric Energy Harvesting (PEH)

2.1.1 Piezoelectricity

A piezoelectric material has mechanical-electrical coupled behavior. PEH is to convert mechanical energy into electric energy. Due to the high energy density and easy installation, PEH is a most popular energy conversion method compared with electromagnetic and electrostatic energy harvesting [2].

Piezoelectric effect can be divided into the following two ways: First, as direct piezoelectric effect, when piezoelectricity is mechanical strained, it can produce corresponding amount of electrical energy as shown in Figure 2-1. Therefore, PEH can be performed based on the piezoelectric effect. Conversely, when the material is applied by electric polarization, the piezoelectric material becomes strained which is called as the inverse piezoelectric effect [3].

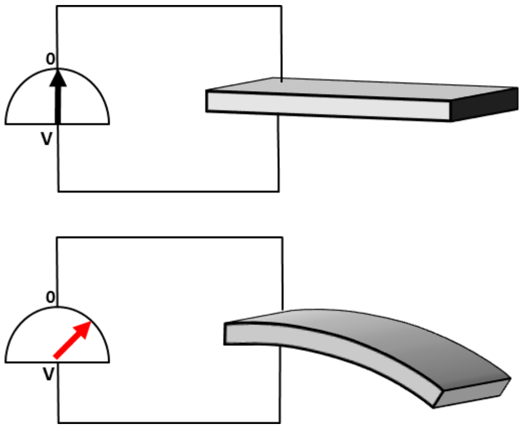

Figure 2-1 Direct Piezoelectric Effect of Piezoelectric Materials [4]

2.1.2 Design Methodologies of Piezoelectric Energy Harvester

From the perspective of the design concept of a piezoelectric energy harvester, many different types of harvester have been presented to efficiently convert energy.

Most common used piezoelectric energy harvester is cantilever-type device which is designed by attaching a single piezoelectric patch (unimorph) or two patches (bimorph) onto the cantilever beam as shown in Figure 2-2. The high mechanical strain and low natural frequency of the cantilever-type harvester make it scavenges high electric energy.

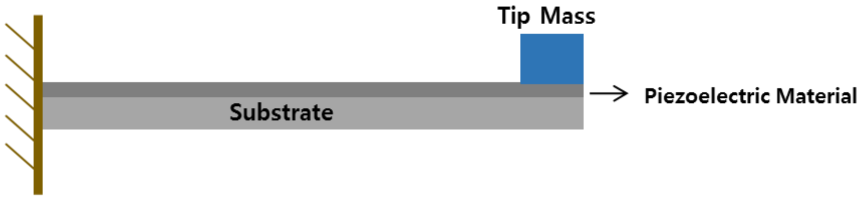

(a)

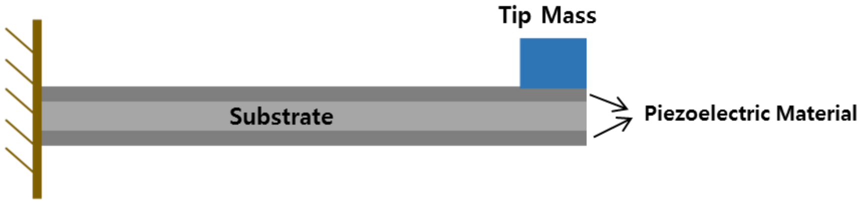

(b)

Figure 2-2 Concept of Cantilever-type Piezoelectric Energy Harvester:

(a) Unimorph and (b) Bimorph

In terms of cantilever beam shape, Frank Goldschmidtboeing and Peter Woias presented analysis with respect to various beam shapes of piezoelectric energy harvester. The experiment validated that shapes has little effect on the overall efficiency, but triangular-shaped beam has more excellent performance than rectangular ones in terms of tolerable excitation amplitude (See Figure 2-3) [5].

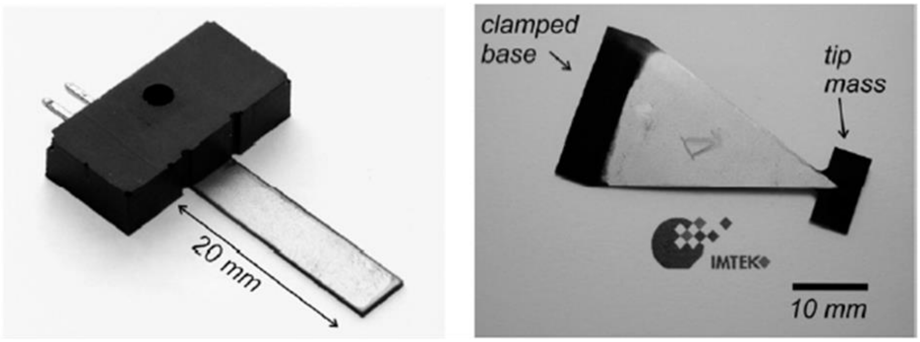

(a) (b)

Figure 2-3 Conventional Cantilevered Energy Harvesters: (a) Rectangular Shape and (b) Triangular Shape [5]

However, cantilever-type energy harvester has some drawbacks at practical applications: 1) proof mass and clamping part of the cantilever-type require more additional space. 2) the device should be insulated from environmental harm such as dirt, moisture, etc. 3) after long-term vibration, the clamping condition becomes loosened, which leads to lose a great deal of vibration energy. In order to overcome these disadvantages, as a compact and durable design, EH skin was proposed by S. Lee and B. D. Youn. Piezoelectric material can be directly attached onto the surface of vibration structure to scavenge electric energy as shown in Figure 2-4 [6].

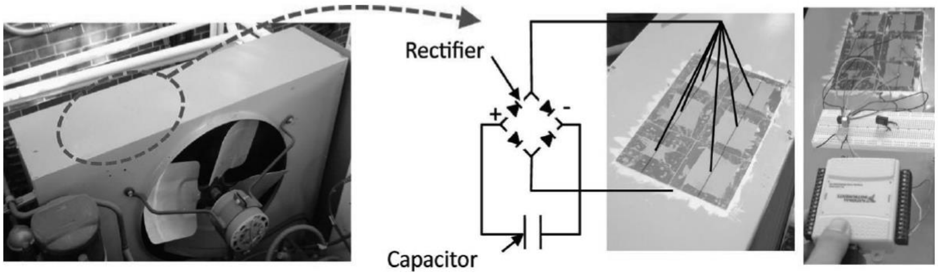

Figure 2-4 Concept of Energy Harvesting Skin (EH Skin) [6]

2.1.3 Piezoelectric Energy Harvesting From Human Activity

Over the past few year, EH almost focused on that scavenges electric power from vibration system. However, as the development of portable devices, to supply the required energy of mobile devices, the concept of PEH from human activities became a significant interest research field. Extensive research effort has been made to scavenge energy from human activities in two ways. One of them is that generate electrical power from continuous human activities such as blood flow [7], breathing [8]. And the other one is from discontinuous activities which include joint and finger motion [9], walking [10] as shown in Figure 2-5.

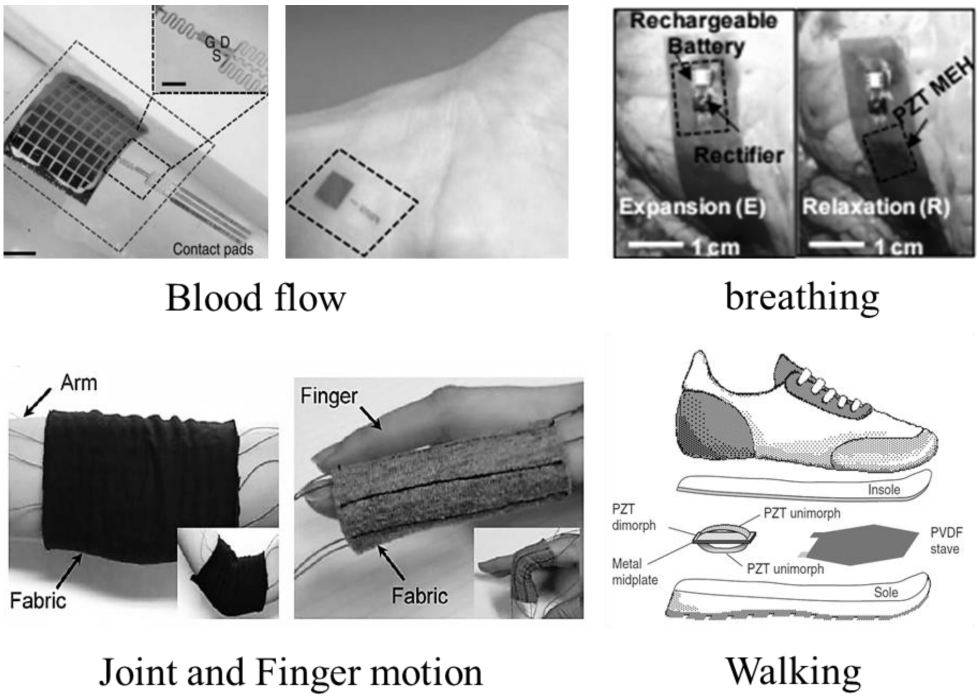

Figure 2-5 Piezoelectric Energy Harvesting from Human Activities [7-10]

As an early work, Starner et al estimated in 1995, heel makes contact with the ground, which is called heel strike has been viewed as the most plentiful source among various human activities. When heel strike is assumed as free fall motion, maximum generated power is 67 W at a brisk pace of two steps per second [11, 12]. In 2004, Penglin Niu et al. presented maximum harvested power is 2W for walking at two steps per second based on the assumption that heel strike isn't performed as a real free motion [13].

2.2 Review of Energy Harvesting Sidewalk Block

Literature review on EH from human activities indicates that walking is a powerful energy source because walking can generate large deformation of the ground. Therefore, energy harvesting sidewalk block has been proposed as an effective energy harvesting application.

There are few energy harvesting sidewalk blocks have been commercialized. One of them is developed from Pavegen company which is the most famous one has been installed in over 100 projects in more than 30 countries (See Figure 2-6 (a)) [14]. Lauren Kemball-Cook has created this system named Pavegen in 2009. This system consists of various shapes blocks containing a piezoelectric system. When people step on the Pavegen tile, if the vertical displacement of the tile is up to 5mm, electric field can be generated for charging a battery or powering a system. The material of top surface of Pavegen tile is 100% recycled tire rubber, and the base is made by 80% recycle materials [15, 16].

The other company called Waydip also has developed a pavement energy harvesting system named Waynergy in 2009. The system is also constructed with many different shapes blocks which contain electric power generation systems. If the vertical displacement is up to 3mm, which is enough to run the electromagnetic system to generate electric energy (See Figure 2-6 (b)) [15, 17].

(a) (b)

Figure 2-6 Commercially Available Energy Harvesting Sidewalk Block:

(a) Pavegen System [14] and (b) Waynergy System [17]

Both of them can be applied on indoor or outdoor pavement, and the generated electric energy is used for charging, wayfinding lighting, street lighting, advertising displays. The location to apply these energy harvesting sidewalk block includes train stations, schools, shopping centers, airport and public place where are high population areas.

Except for Pavegen system and Waynergy system, Innowattech Ltd in Israsel and Senbool Inc in Republic of Korea have also developed their own energy harvesting sidewalk block systems. However, all commercially available products have not developed based on a scientific approach. Little effort has been made about how to response human walking mechanism into the design concept and how to obtain a high reliable design. Thus, in this thesis, a systematic design methodology of energy harvesting sidewalk block is proposed to overcome the above challenges

Chapter 3. Human Gait Analysis

Gait analysis is a systematic study to investigate human walking motion. The research on human walking began in 17th century in Europe [18]. In 1682, Borelli first measured the center of gravity (C.G) of human body and proposed how human body maintains balance when walking forward constantly. Afterwards, Weber brothers presented clear description about gait cycle in 1836 in Germany.

Extensive researches have been made from various points of view such as kinematic measurement, mechanical analysis, mathematical modeling, muscle activity, force platforms, and clinical application [19].

In this thesis, for the purpose of designing an energy harvesting sidewalk block while accounting human walking characteristics, human gait analysis has been investigated to extract a loading profile from ground reaction force. In Chapter 3, human gait analysis is introduced. In Section 3.1, a brief review on human gait cycle is provided. Furthermore, Section 3.2 describes ground reaction force during gait cycle.

3.1 Gait Cycle

One of the important terminologies used in gait analysis is gait cycle which is a duration from the initial ground contact of one foot to the next contact of the same foot. As shown in Figure 3-1, gait cycle is defined, which begins at the initial contact of the right foot and ends at the instant that right foot contacts ground again.

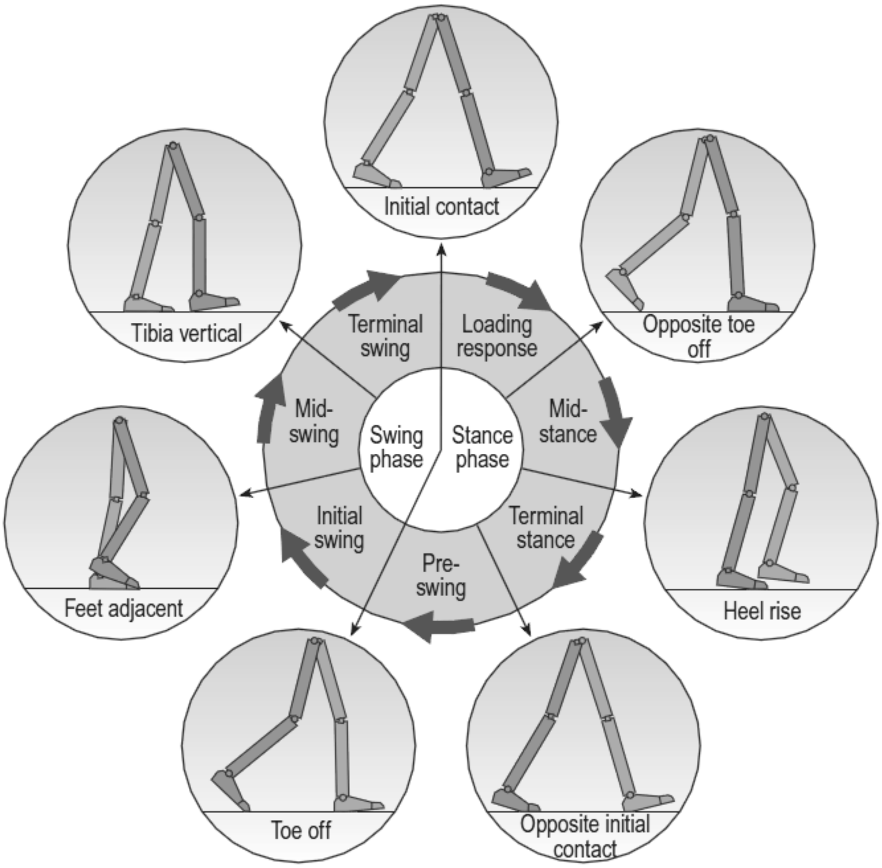

Figure 3-1 Gait Cycle [19]

Gait cycle can be generally divided into two phase: Stance phase and Swing phase. In single gait cycle, stance phase takes up 60% of the full gait cycle, and swing phase takes up the remaining 40%. Stance phase is also called as "support phase" or "contact phase". It is a period lasts from initial contact (heel strike) to the toe off. Stance phase can be subdivided into four parts:

(1) Loading response:

A time interval between the initial contact of supporting foot (right) and opposite toe off (left). Center of gravity moves to the supporting foot (right) at this period.

(2) Mid-stance:

A period is from opposite toe off (left) to heel rise of supporting foot (right), and center of gravity is on the supporting foot (right).

(3) Terminal stance:

It begins when center of gravity is over the supporting foot (right) and ends when the opposite foot (left) contacts to the ground.

(4) Pre-swing:

It starts with the initial contact of the opposite foot (left) and ends at the toe off of the supporting foot (right). Body weight transfers to the opposite foot.

Because the supporting foot remains contact with the ground during stance phase, characteristics of stance phase is main research part when design energy harvesting sidewalk block.

Swing phase is also a time interval when the foot is off the ground and limb swings forward through the air. It contains the following three parts:

(1) Initial swing:

It begins when the right foot is lifted from ground and ends when the right swing foot is opposite to the left stance foot.

(2) Mid-swing:

It starts at the end of initial swing and ends when the right foot is in front of the body.

(3) Terminal swing:

A duration between the end of mid-swing and the ground contact of right foot.

Gait cycle is also known as cycle time from the view of time concept, which can be divided into stance time and swing time. The timing of gait cycle is described in Figure 3-2.

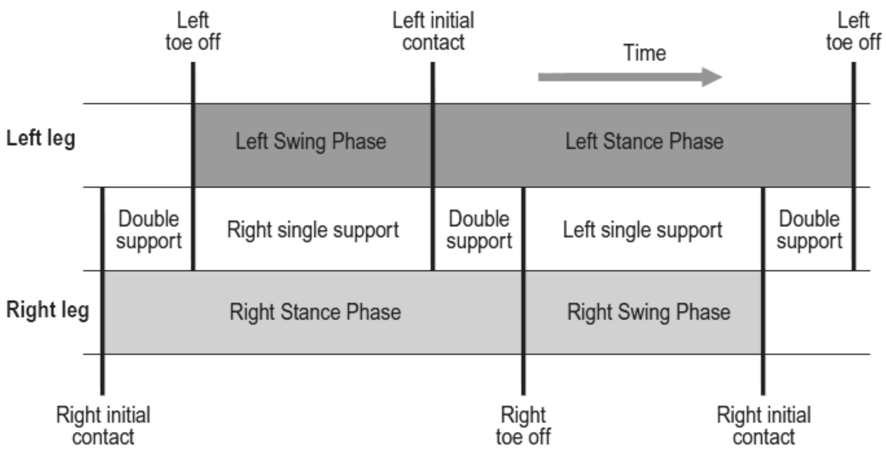

Figure 3-2 Single Support and Double Support During Gait Cycle (Cycle Time) [19]

The cycle starts with initial contact of right foot, at the same time left foot always remains contact with the ground, this period thus is a double support period. And, the period of single support begins when the left foot toes off, only the right foot is still on the ground as shown in Figure 3-2 [19].

3.2 Ground Reaction Force

In 1950, Bresler and Frankel presented free-body calculations about limb segment, which allowed for producing ground reaction force (GRF). Since the past 20 years, many studies have been published with respect to ground reaction force with time histories. The instrument called force plate is a standard equipment for measuring ground reaction force. Amar in 1924 firstly designed the force plate, and Elftman in 1938 improved it. Even though few force plates just give vertical component of force, most of them provide three component force information (vertical, medio-lateral and anter-posterior) as shown in Figure 3-3. Ground reaction force is produced when people walk on the platform, which provides elementary information including magnitude, direction along the center of pressure path beneath the foot as shown in Figure 3-4. The resultant force is a combination of many small forces which scattered at the contact area. Generally, compared among three component, vertical force is the dominate one. The vertical force is generated from initial heel contact to the toe off to assist finding stance phase [19-21].

Figure 3-3 shows an experiment result which had 18 males aged from 18 to 38 years old volunteers, and their mean mass was 78.3 kg. Each of the volunteers had their own self-selected pace, and the mean walking velocity was 1.6 m/s. In addition, every volunteer had ten walking trails, but the recorded one was that the participant stepped fully on the force plate. The output ground reaction force was averaged value and normalized by body weight [21].

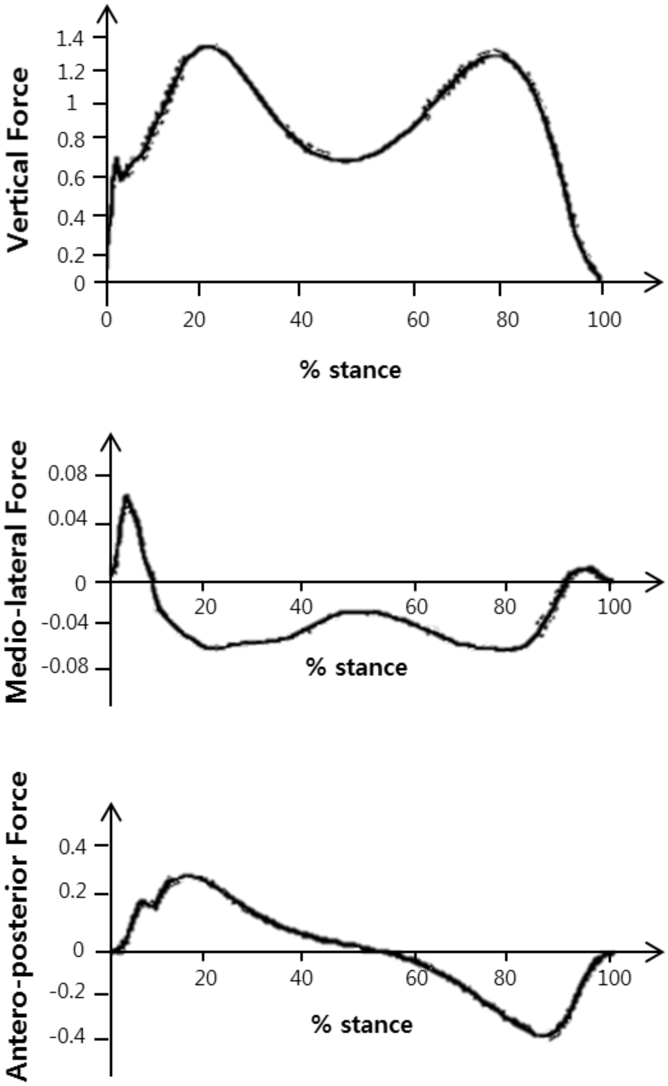

Figure 3-3 Ground Reaction Force at Vertical, Medio-lateral, and Anter-posterior Forces [21]

EH sidewalk block is designed based on the vertical component of ground reaction force because vertical force dominantly leads to the deformation of ground. As shown in Figure 3-3, vertical force seems like a double hump with an initial small peak. The initial small peak is produced by heel strike. The first hump is a result of upward acceleration by the movement of center of gravity at early stance phase. And, the middle hollow is the response of mid-stance. The second peak is made by the deceleration in late stance phase [19] .

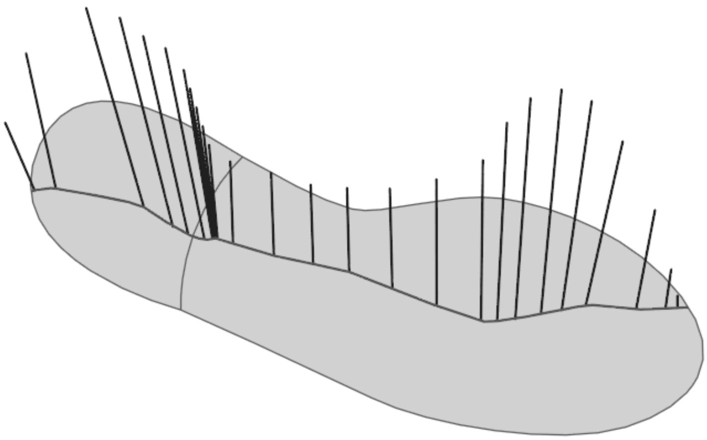

Figure 3-4 Ground Reaction Force along Center of Pressure [19]

Chapter 4. Conceptual Design of Omnidirectional Energy Harvesting Sidewalk Block

For developing design of energy harvesting sidewalk block, loading condition and voltage cancellation effect are considered in this thesis. Loading condition consists of foot size, loading profile, foot position and direction, which is described in Section 4.1. In order to avoid voltage cancellation effect, piezoelectric material segmentation methodology is applied to design piezoelectric patch, which is depicted in Section 4.2. As a result, in Section 4.3, shape design of energy harvesting sidewalk block is proposed.

4.1 Loading Condition

4.1.1 Foot Size

The whole design process of energy harvesting sidewalk block in this study is conducted based on average male in Republic of Korea. Average mass of male is 70 kg, length and width of the foot are 27 and 10 cm, respectively as shown in Figure 4-1.

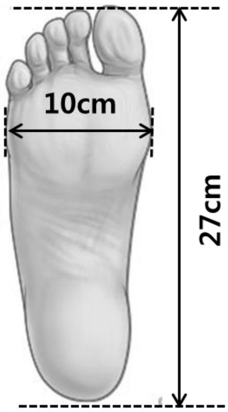

Figure 4-1 Foot Size

4.1.2 Loading Profile

Based on the research of normalized GRF [21], loading profile is extracted according to the average mass as shown in Figure 4-2.

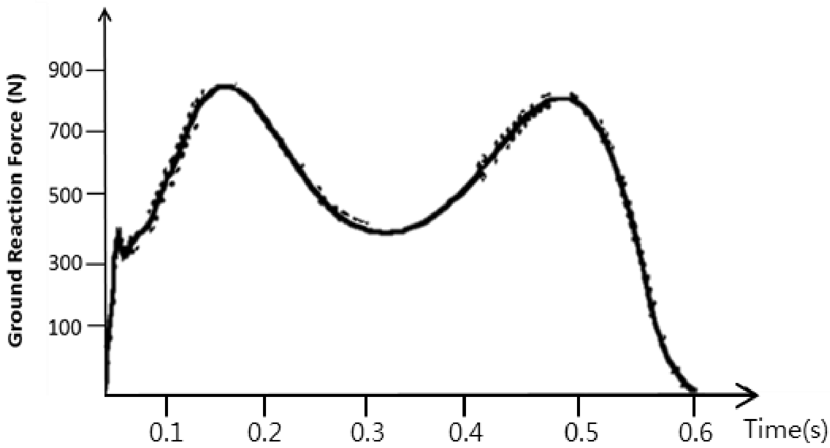

Figure 4-2 Loading Profile

Since the average human walking speed is approximately 1 m/s [19], stance phase begins at the initial contact of foot and sustains to 0.6 s, because stance phase accounts for 60 % of whole gait cycle.

4.1.3 Footstep Position

In this thesis, the omnidirectional energy harvesting sidewalk block is designed as a square with size of 50 cm $\times$ 50 cm. A pedestrian just walks on center of the energy harvesting sidewalk block as shown in Figure 4-3. Therefore, the variation of a footstep position is not considered in this thesis.

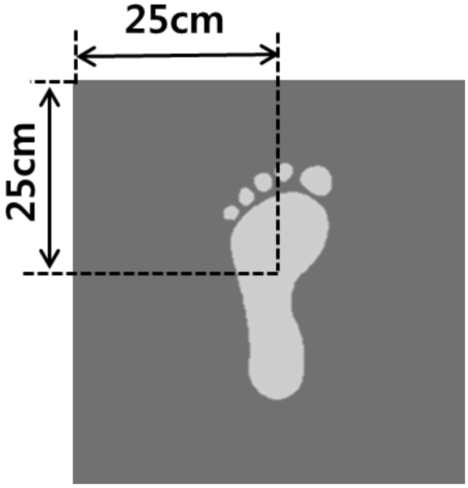

Figure 4-3 Footstep on Center of the Sidewalk Block

4.1.4 Footstep Direction

Directional randomness of footstep is also an important assumption in this study

(See Figure 4-4). The angle range of footstep is from 0 to 360 degree. Therefore, this thesis proposes an omnidirectional energy harvesting (OEH) sidewalk block concept to generate sufficient output energy at all the direction of footstep.

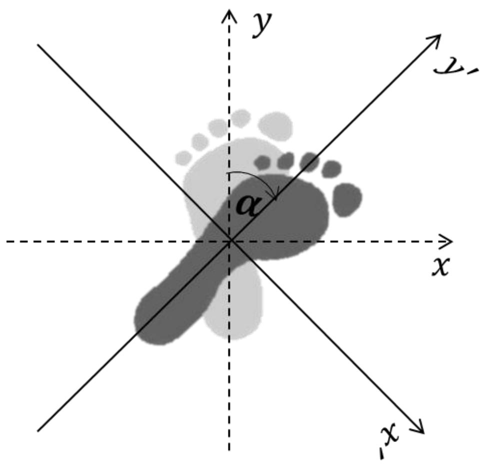

Figure 4-4 Directional Randomness of Footstep

4.2 Piezoelectric Material Segmentation

In this study, OEH sidewalk block is fully clamped at *x, y, z* axis. When people step on the center of sidewalk block, strain sign of center and edge will be opposite, which results in voltage cancellation occurs at inflection line.

Thus, piezoelectric material segmentation methodology is applied when design piezoelectric patch to avoid voltage cancellation effect by eliminating piezoelectric material at inflection line as shown in Figure 4-5 [22]

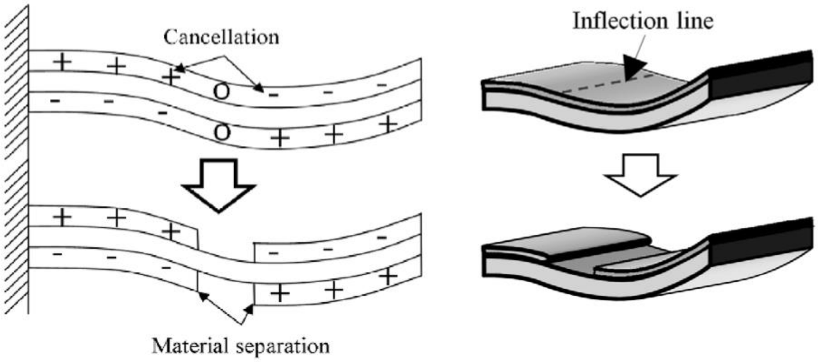

Figure 4-5 Piezoelectric Segmentation Design [22]

4.3 Shape Design of Omnidirectional Energy Harvesting Sidewalk Block

Shape design of OEH sidewalk block is proposed by considering above assumptions. The sidewalk block is constructed by two layers. The base layer is called as substrate in this thesis, designed by structural steel. A common used piezoelectric material - PZT-5H4E is selected to make top layer due to the high electromechanical coupling coefficient, which are attached on the substrate using adhesive material. In addition, the top and bottom electrodes of piezoelectric patches are connected with external electrical resistance as an electrical circuit as shown in Figure 4-6. Therefore, when people walk on the substrate, the deformation of attached piezoelectric patch generates electric energy to power the external electric device.

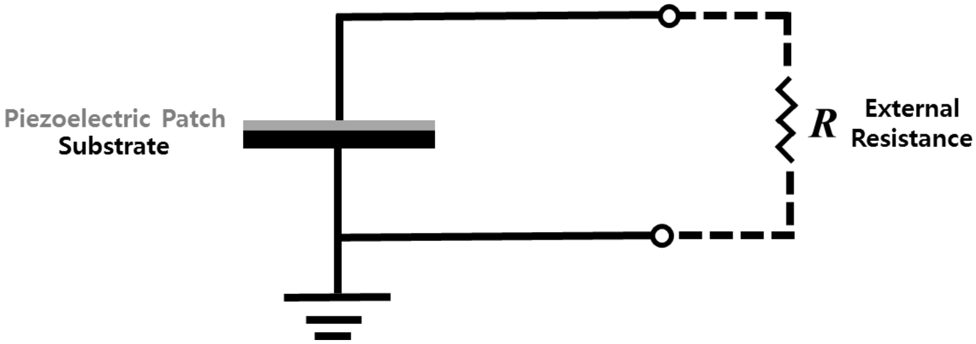

Figure 4-6 External Circuit of OEH Sidewalk Block

As shown in Figure 4-7, OEH sidewalk block is composed of one large square substrate, four edge piezoelectric patches and eight center piezoelectric patches. And, the substrate is fully clamped at *x, y, z* axis.

The four edge patches are determined by material segmentation methodology of EH skin because when people step on the center of sidewalk block, compression occurs at the center, and while tension happens on the edge of substrate. Furthermore, in order to cover the omnidirectional footstep, center piezoelectric patches are designed like a whole piece of doughnut shape. However, since the largest fabrication size of piezoelectric patch is 10 cm, it is not large enough to manufacture the whole piece of doughnut shape. Therefore, the doughnut shape has to be divided into eight piezoelectric patches.

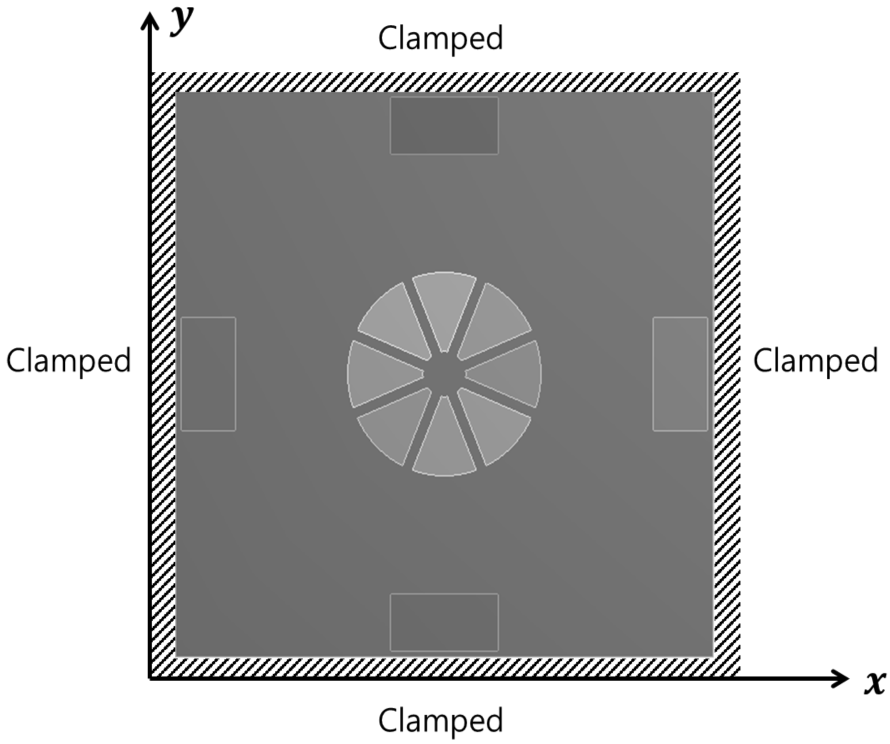

Figure 4-7 Geometry of OEH Sidewalk Block

Chapter 5. Multiphysics Simulation under Transient Footstep Loading

In this study, human gait simulation is implemented by multiphysics analysis using ANSYS® Workbench™ R15.0, which includes transient analysis and piezoelectric-circuit analysis. Chapter 5 provides detail procedure of multiphysics analysis from model construction to final analysis of output result. In Section 5.1, finite element modeling of OEH sidewalk block is described. Furthermore, mechanical stress of OEH sidewalk block, output voltage and energy are explained in Sections 5.2 and 5.3 sequentially.

5.1 Multiphysics Analysis Using Finite Element Method

5.1.1 Modeling Approach

The finite element modeling of OEH sidewalk block is constructed using three elements as shown in Figure 5-1. Substrate is modeled by SOLID 186. The top piezoelectric patches are modeled using SOLID226 element. This element is useful to model 3-D coupled-field solid, which has twenty nodes, up to five degrees of freedom per node. In terms of piezoelectric material, SOLID 226 indicates four coupled degrees of freedom. One of them is electric potential difference between top and bottom electrodes, the other are three translational displacements (UX, UY and UZ). VOLT degree of freedom per node on the top surface of piezoelectric patch are coupled to be a top electrode, and the top surface of substrate is defined as bottom electrode which is ground (zero electric potential). These two electrodes are connected with an external electrical resistance using CIRCU 94 element which is employed for piezoelectric-circuit analyses. Furthermore, four edge of OEH sidewalk block are fully clamped.

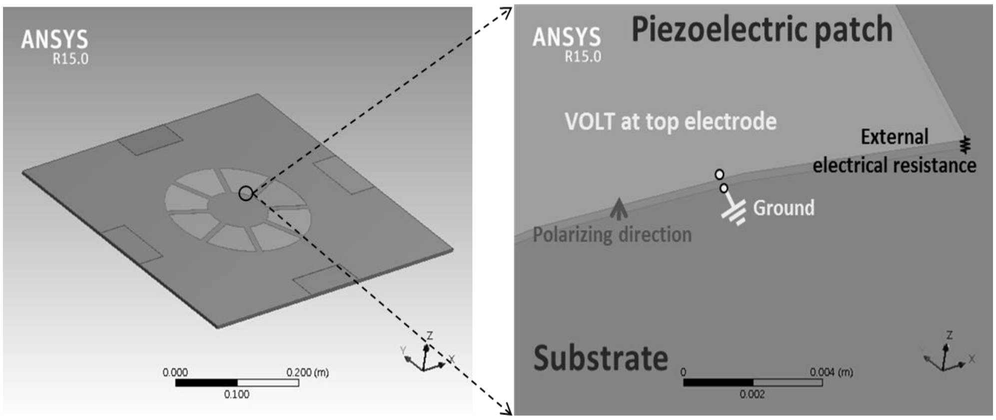

Figure 5-1 Finite Element Modeling of Omnidirectional Energy Harvesting Sidewalk Block

In terms of material properties, mechanical properties of the piezoelectric patch and the substrate are summarized in Table 1 [23, 24]. And, Table 2 summarizes the electrical properties of the piezoelectric patch [24].

Table 1 Mechanical Properties of the Piezoelectric Patch (PZT-5H4E) and the Substrate (Structural Steel)

Piezoelectric patch (PZT-5H4E)	Compliances	s_{11}	16.5E-12 m^2/N
		s_{12}	-4.78E-12 m^2/N
		s_{13}	-8.45E-12 m^2/N
		s_{33}	20.7E-12 m^2/N
		s_{44}	43.5E-12 m^2/N
		s_{66}	42.6E-12 m^2/N
	Poisson's ratio	ν_p	0.34
	Density	ρ_p	7500 Kg/m^3
Substrate (Structural Steel)	Young's modulus	Y_s	2E+11 Pa
	Poisson's ratio	ν_s	0.30
	Density	ρ_p	7850 Kg/m^3

Table 2 Electrical Properties of the Piezoelectric Patch (PZT-5H4E)

Piezoelectric strain coefficient	d_{31}	-274×10^{-12} m/V
Piezoelectric constant	$\overline{e}_{31}$	-6.62 C/m^2
Absolute permittivity	ε_0	8.85×10^{-12} F/m
Dielectric permittivity at constant stress	ε_{33}^T	30.10×10^{-9} F/m
Dielectric permittivity at constant strain	ε_{33}^S	17.29×10^{-9} F/m
Relative permittivity (relative dielectric constant)	ε_r	3400

5.1.2 Gait Simulation Using Transient Analysis

Transient analysis is performed to simulate human gait in this study. As a loading condition, the extracted loading profile – ground reaction force (See Figure 4-2) is divided into 17 steps. Each step force is applied using nodal force on the corresponding selected position as shown in Figure 5-2. Since ground reaction force is generated along center of pressure, the forced position is also moved along center of pressure.

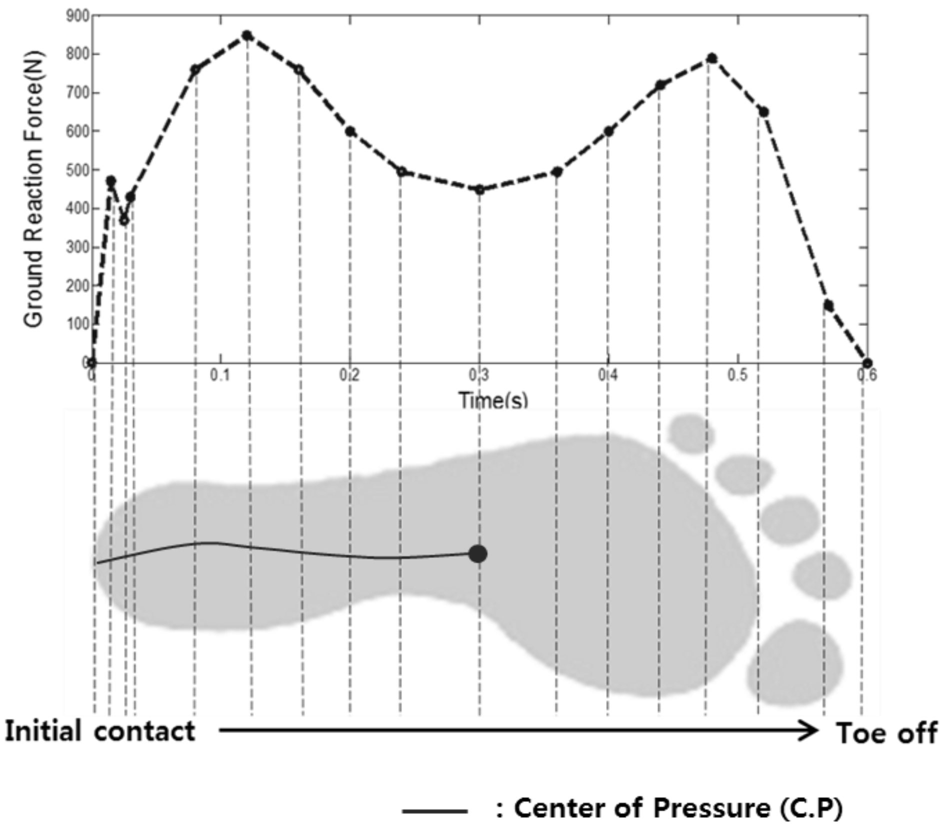

Figure 5-2 Loading Profile in Transient Analysis

5.2 Stress Result in Transient Analysis

Maximum Principal stress of piezoelectric patch (brittle material) and von-Mises stress of substrate (ductile material) at 0.12s are plotted in Figure 5-3 and Figure 5-4, respectively. Strain distribution of OEH sidewalk block is also plotted in Figure 5-5. Since heel strike generates maximum ground reaction force during stance phase occurring at 0.12s, the maximum deformation of OEH sidewalk block thus happens at that moment. The results will be updated when design variables of

OEH sidewalk block are changed. The strain of OEH sidewalk block directly responses to output voltage. The maximum stress values are considered as fatigue failure constraints when design a reliable OEH sidewalk block.

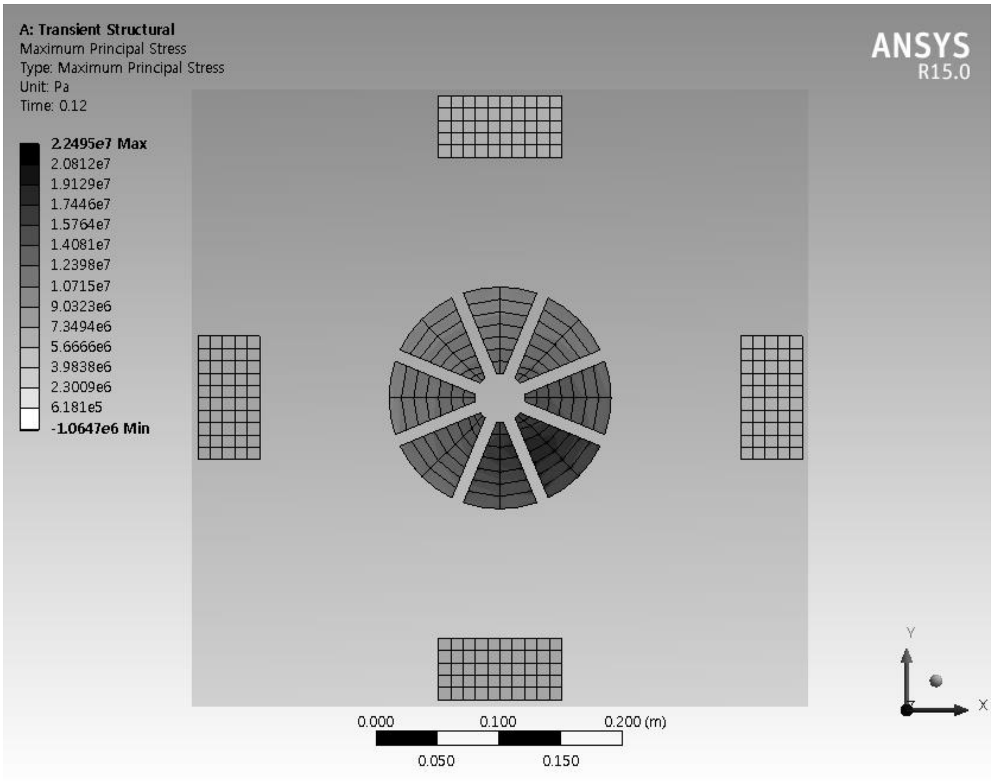

Figure 5-3 Maximum Principal Stress of Piezoelectric Patch at 0.12s

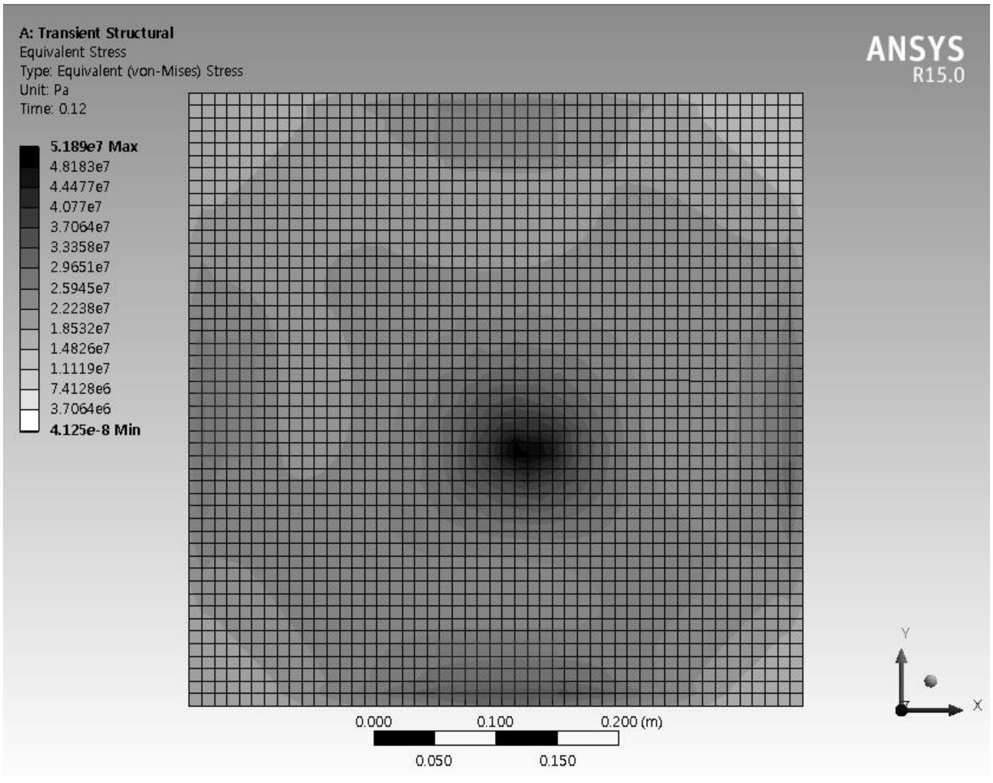

Figure 5-4 von-Mises Stress of Substrate at 0.12s

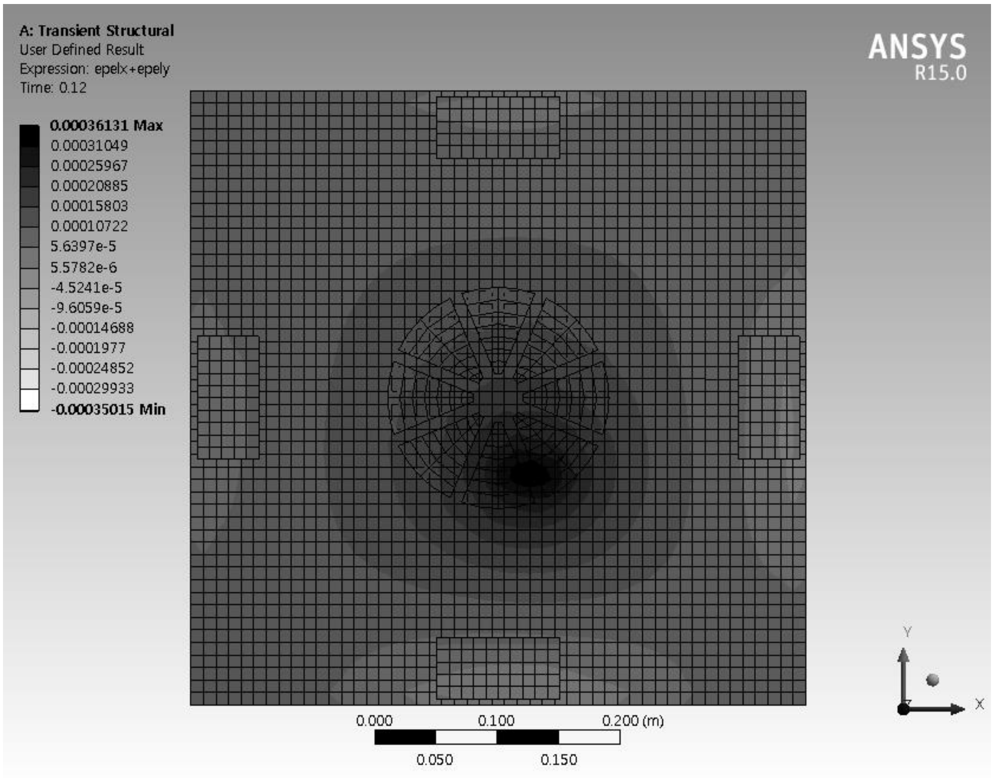

Figure 5-5 Strain Distribution of OEH Sidewalk Block at 0.12s

5.3 Output Voltage and Energy in Transient Analysis

In terms of piezoelectric-circuit analysis, the voltage and energy result with respect to various external resistances are plotted in Figure 5-6 and Figure 5-7, respectively.

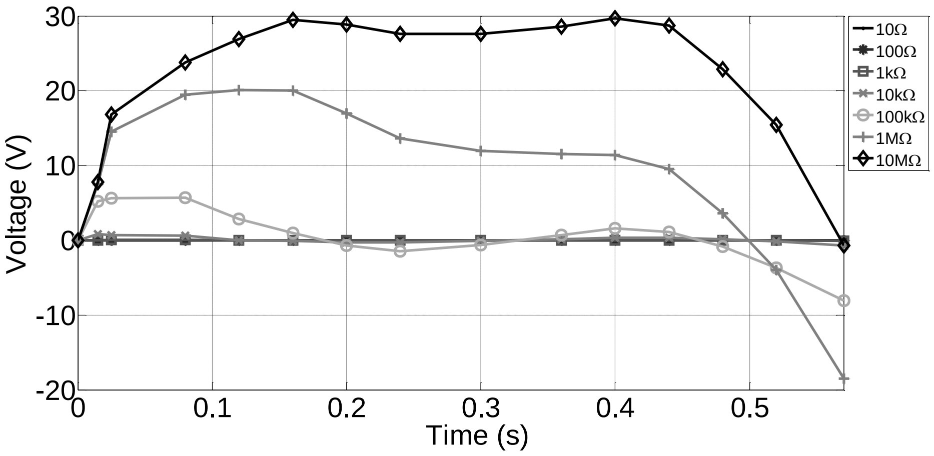

Figure 5-6 Time-variant Output Voltage with respect to Various Resistances

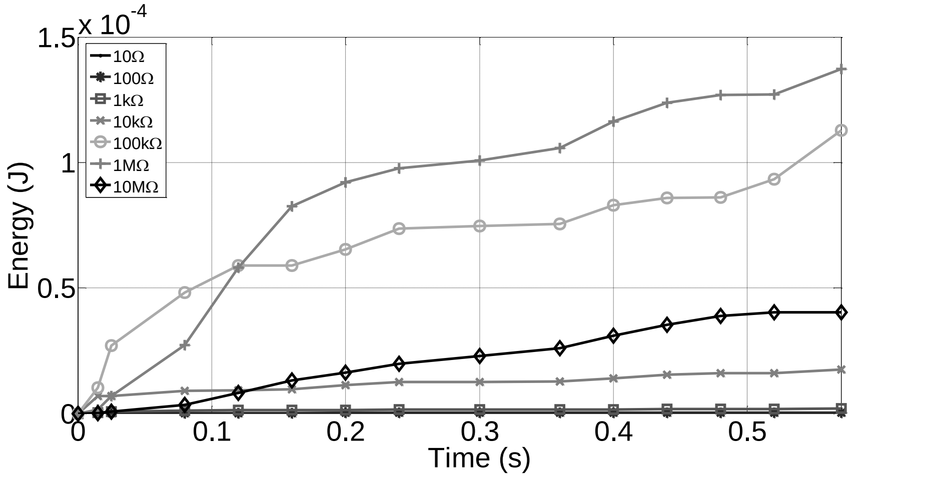

Figure 5-7 Time-variant Output Energy with respect to Various Resistances

The result of voltage indicates that dissipation of voltage happens at stance phase, and the degree of dissipation is different according to value of external resistance. Therefore, different trends of voltage and energy with respect to various resistance are obtained.

The reason caused this phenomenon is that resistance – capacitor (RC) circuit is established when piezoelectric material connects with external resistance as shown in Figure 5-8 [25]. RC circuit has its own typical phenomenon – time constant as written in Eq. (5.1), which causes electrical damping under transient loading condition.

$$\tau = RC \tag{5.1}$$

$$C = \frac{\bar{\varepsilon}_{33}^{S} A}{h_p} \tag{5.2}$$

where τ is time constant, R is external resistance, C is capacitance of piezoelectric patch. Capacitance of piezoelectric patch is explained using Eq. (5.2), which consists of relative permittivity at constant strain $\bar{\varepsilon}_{33}^{S}$, area of piezoelectric patch A, and thickness h_p of patch. Since permittivity and thickness are constant values, and capacitance is changed by the area of patch, time constant is determined by area of piezoelectric path and external resistance in this thesis.

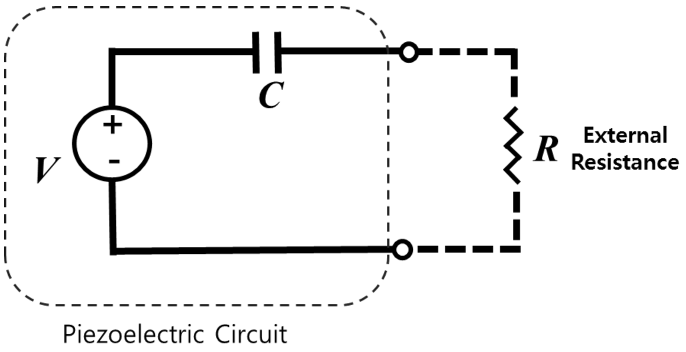

Figure 5-8 Equivalent Circuit Model of Piezoelectric Patch with External Resistance

Consequently, when design OEH sidewalk block, external resistance and area of piezoelectric patch are defined as two important design variables to scavenge high electric energy.

.

Chapter 6. Reliability-Based Design Optimization of Omnidirectional Energy Harvesting Sidewalk Block

Deterministic design optimization does not consider physical uncertainty in the material properties and manufacturing tolerance which can affect the output energy and mechanical stress of OEH sidewalk block, finally it could result in unreliable design. Therefore, it is of critical important to analyze the uncertainty propagation. For the purpose of addressing this challenge, RBDO is executed to reliably scavenge output energy from human gait while accounting for various physical uncertainties. In this thesis, as a design process of OEH sidewalk block, after obtaining the solution of deterministic design optimization (DDO) first, reliability-based design optimization (RBDO) is sequentially launched starting at the point of deterministic optimum design. Compared with DDO, RBDO can obtain a reliable solution of OEH sidewalk block in a probabilistic manner by using statistical information of a loading condition geometry, and material properties.

Chapter 6 presents how to perform design optimization of OEH sidewalk block. In section 6.1, design formulations with a design optimizer and reliability analysis are depicted. The random design and noise variables and the corresponding design bounds are defined in Section 6.2. In addition, the surrogate model construction for efficiently performing RBDO is explained in Section 6.3. As a result, the final design configuration of OEH sidewalk block and relevant information are presented in Section 6.4.

6.1 Design Formulation

6.1.1 Deterministic Design Optimization

Deterministic design optimization of OEH sidewalk block can be formulated as follows:

$$\begin{aligned} &\text{Maximize} \quad E(\mathbf{d}) \\ &\text{subject to} \quad G(\mathbf{d}) < 0 \\ &\qquad \mathbf{d_L} \le \mathbf{d} \le \mathbf{d_{U,}} \quad \mathbf{d} \in R^{nd} \\ &\qquad where \;\; G(\mathbf{d}) = \sigma_{PZT}(\mathbf{d}) - \sigma_e \end{aligned} \tag{6.1}$$

where $E(\mathbf{d})$, $\mathbf{d} = [d_i]^T$, and *nd* represent the electrical energy, the design vector, the number of design variables, respectively. The output energy indicates the sum of output energy of eight center piezoelectric patches. $\mathbf{d_L}$ and $\mathbf{d_{U,}}$ are the lower and upper bounds of design variables. $G(\mathbf{d})$ is a performance constraint which is defined as the subtraction of the fatigue strength of piezoelectric patch (σ_e) from Maximum Principal stress (σ_{PZT}). The fatigue strength of piezoelectric patch is 48.3 MPa [26].

6.1.2 Reliability-Based Design Optimization

Reliability-Based Design Optimization can be formulated as follows:

$$\begin{aligned} &\text{Maximize} \quad E(\mathbf{d}) \\ &\text{subject to} \quad P\{G\{\mathbf{X};\mathbf{d}(\mathbf{X})\} < 0\} > R_t \\ &\qquad \mathbf{d_L} \le \mathbf{d} \le \mathbf{d_{U,}} \quad \mathbf{d} \in R^{nd} \text{ and } \mathbf{X} \in R^{nr} \\ &\qquad where \;\; G\{\mathbf{X};\mathbf{d}(\mathbf{X})\} = \sigma_{PZT}(\mathbf{X};\mathbf{d}(\mathbf{X})) - \sigma_e \end{aligned} \tag{6.2}$$

where *nr* is the number of random variables, and $\mathbf{X} = [X_i]^T$ is the random vector. In RBDO, the design problem is formulated as maximization of output energy subjected to fatigue failure constraint of piezoelectric patch in probabilistic manner. The probabilistic constraints are described by the performance function $G\{\mathbf{X}; \mathbf{d}(\mathbf{X})\}$, and target reliability R_t is defined as 99.87%.

In this, thesis, RBDO is performed by double loop approach. Design optimization is implemented by Progressive Quadratic Response Surface Method (PQRSM) and reliability analysis is conducted by Monte-Carlo Simulation (MCS).

<u>Progressive Quadratic Response Surface Method (PQRSM)</u>

PQRSM is one of the sequential approximate optimization (SAO) algorithms. PQRSM is a useful method to deal with high computational costs and numerical noise of problem. The steps of PQRSM are as follows.

- Step 1) Define the initial design space, which is assumed to 30% ~ 50% of the whole design space, and includes the initial design value.
- Step 2) Choose 2*n*+1 sampling points within the design space.
- Step 3) Build approximate model using quadratic polynomial approximation.
- Step 4) Perform approximate optimization
- Step 5) Evaluate actual objective and constraints at the approximate optimum
- Step 6) Check convergence or not at the approximate optimum by using actual objective and constraints. If the convergence criteria are satisfied, it will stop, otherwise update the trust region, go to step 2.

Monte Carlo simulation (MCS)

Since numerous failure modes exist in engineering systems, reliability analysis should be conducted by probabilistic approach to evaluate the performance of system. In this thesis, the fatigue failure of the piezoelectric patch is considered as the failure mode of OEH sidewalk block. Among various methods of reliability analysis, MCS, one of widely used random sampling methods, is performed in this study. In order to evaluate the reliability, MCS is performed as follows

- Step 1) Random input samples are generated based on the corresponding probability distribution functions
- Step 2) Output result of the model are calculated, check if the system has failed or not.
- Step 3) Repeat from steps 1 to 2 number of times (N), count the number of failures (N_f).
- Step 4) Calculate the probability of failure (p_f) [27, 28]. Finally, the reliability can be obtained as $1-p_f$.

$$p_f = \frac{N_f}{N} \tag{6.3}$$

6.2 Definition of Design and Noise Variables

6.2.1 Design and Noise Variables

In this thesis, four design variables - external resistance (R), inner radius (r_i) and outer radius (r_o) of doughnut shape, and thickness of substrate (t) are defined. Furthermore, except for external electrical resistance, the other three design variables are assumed as random variables. The properties of design variables are summarized in Table 3. All random design variables are assumed to be statistically modeled as normal distribution.

Table 3 Properties of Design Variables

Design Variable	Classification	Mean	COV	Lower bound	Upper bound
r_i [m]	Random	0.0375	0.01	0.025	0.05
r_o [m]	Random	0.1125	0.01	0.1	0.125
t [m]	Random	0.0035	0.01	0.002	0.005
R [kΩ]	Deterministic	495	-	10	1000

In addition, Young' modulus of structural steel (Y_s), piezoelectric constant (e_{31}), elastic modulus (c_{11}), and the direction of footstep (α) which directly affect the output voltage and mechanical stress of OEH sidewalk block are selected as noise variables. The properties of noise variables are summarized in Table 4 [23, 24] .

Table 4 Properties of Noise Variables

Noise Variable	Mean	COV	Distribution Type
Y_s [GPa]	200	0.05	Normal
e_{31} [C/m^2]	-6.6228	0.05	Normal
c_{11} [GPa]	127.205	0.05	Normal
α [rad]	3.14	0.33	Uniform

6.2.2 Bound of Random Design Variables

The bounds of radius, thickness of substrate, external electrical resistance are defined as follows.

1) Radius of doughnut shape:

The bounds of inner and outer radius are determined by considering two aspects. First, the smallest size of piezoelectric patch should also cover the whole area of maximum strain. Second, the size of sector should be smaller than largest fabrication size (10cm) of PZT-5H4E.

2) External electrical resistance:

With respect to bounds of external electrical resistance, it is decided by preliminary research that the maximum output energy can be obtained in the range of 10 kΩ to 1 MΩ as shown in Figure 5-7.

3) Thickness of substrate:

In order to define the bound of thickness of substrate, sensitivity analysis are performed with respect to thickness of substrate. The result of analysis are listed in Table 5.

Table 5 Sensitivity Analysis with respect to Various Thicknesses of Substrate

Thickness [mm]	**1**	**2**	**3**	**4**	**5**	**6**
Maximum Principal Stress of Piezoelectric Patches[MPa]	181	107	62.6	36.1	22.8	15.7
Maximum von-Mises Stress of Substrate [MPa]	435	246	142.3	82.1	52.6	36.7
Maximum Output Energy[J]	0.04	0.02	0.01	0.004	0.002	0.0007

The sensitivity analysis result indicates the fatigue strength of piezoelectric patch (48.3MPa) [23] might be occurred at around 3.5mm, and fatigue strength of structural steel (230MPa) [29, 30] happened at around 2mm. Therefore, in order to have enough feasible region for RBDO, the bound of thickness is defined from 2mm to 5mm.

According to above research, the bounds of four design variables are summarized in Table 3.

6.3 Surrogate Model Construction

6.3.1 Design of Experiment

In order to save computational cost, surrogate model is constructed based on design of experiment (DOE). An optimal samples which have high relativity can be obtained in the design space using DOE method. A variety of sampling methods have been developed until now such as Central composite design, Box-Behnken, Latin Hypercube, and Orthogonal Arrays. In this thesis DOE is performed by using Latin hypercube sampling (LHS) method. LHS is one of space-filling techniques, which follows a Latin square where only one sample generates in each row and each column. All the samples can be uniformly distributed in the space of a surrogate model by using LHS [31-33].

With respect to the bounds of DOE, except for deterministic design variable, both of the random design and noise variables use target reliability (3 times standard deviation) to define the bounds of DOE as shown in Figure 6-1.

In the case of random design variables, the bounds of DOE should be larger than the design space (gray) by a factor of 3 times standard deviation so as to cover the whole design space. $\mu_i^{\mathrm{d,L}}$ and $\mu_i^{\mathrm{d,U}}$ are the mean values of the random design variables at lower and upper design bounds.

In the case of noise variables, the bounds of DOE is from the mean value to the points of a factor of 3 times standard deviation, where μ_i is the mean value of a random noise variable. The denotation σ_i is a standard deviation of design and noise variables. The final bounds of DOE about design and noise variables are summarized in Table 6 and Table 7, respectively.

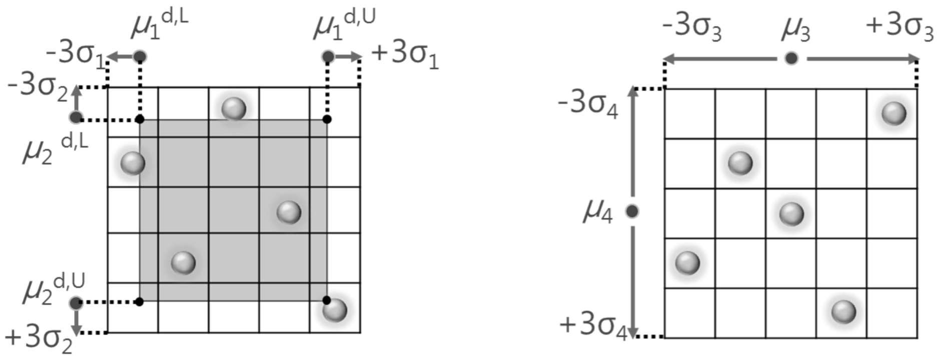

(a) (b)

Figure 6-1 Bounds of (a) Design Variables and (b) Noise Variables

Table 6 DOE Bound of Design Variables

Design Variable	Lower bound	Upper bound
r_i [m]	0.02425	0.0515
r_o [m]	0.097	0.12875
t [m]	0.00194	0.00515
R [kΩ]	50	1000

R: External resistance is deterministic design variable

Table 7 DOE Bound of Noise Variables

Noise Variable	Lower bound	Upper bound
Y_s [GPa]	170.00	230.00
e_{31} [C/m^2]	-7.62	-5.63
c_{11} [GPa]	108.12	146.28
α [rad]	0	6.28

The number of training points using LHS method in terms of large-scale problem is defined as follows [33]:

$$\text{The Number of Training Point} = \frac{3(i+1)(i+2)}{2},\ (i=8) \tag{6.4}$$

where i is number of variables including four design variables and four noise variables.

To avoid the nonuniform distribution caused by different scale of variables, variables normalization is perform as follows:

$$\tilde{x}_i = \frac{x_i - x_{i,\min}}{x_{i,\max} - x_{i,\min}} \tag{6.5}$$

where $\tilde{x}_i$ is normalized value, and the denotation x_i, $x_{i,\min}$, $x_{i,\max}$ are physical value, physical minimum and maximum values, respectively.

After the above procedure, 135 training points are obtained based on LHS method.

6.3.2 Candidates of Surrogate Model

In this thesis, commercial optimization software - PIAnO is used to perform design optimization with surrogate model by connecting ANSYS® Workbench™. PIAnO software provides eleven types of surrogate models based on Polynomial Regression (PR), Kriging (KG), Radial Basis Functions (RBF), which are listed in Table 8.

Table 8 Candidates of Surrogate Models in PIAnO

Polynomial Regression	**Kriging**	**Radial Basis**
Constant	Constant	-
Linear	Linear	
Simple Quadratic	Simple Quadratic	
Full Quadratic	Full Quadratic	
Simple Cubic	Simple Cubic	

(1) Polynomial Regression:

Polynomial model is often used to distinguish the importance of each design variable from the coefficients, and attempt to obtain the most critical one. The advantage of this model is quick convergence in terms of noisy function. However, it has limitation when expresses high nonlinear problem.

The most common used second-order polynomial model can be expressed as follows:

$$\hat{y} = \beta_o + \sum_{i=1}^{k} \beta_{ii} x_i^2 + \sum_i \sum_j \beta_{ij} x_i x_j \qquad (6.6)$$

where β_o, β_{ii}, β_{ij} are coefficients of polynomial, and x_i, x_j are design and noise variables in this thesis [33].

(2) Kriging:

Since the Kriging can have wide range of correlation function, it has high flexibility. However, when construct the model, it has drawback of high time-consuming.

The model is composed of fixed function $f_j(x)$ and stochastic process forms as follows:

$$\hat{y} = \sum_{j=1}^{k} \beta_j f_j(x) + Z(x) \qquad (6.7)$$

$$\mathrm{cov}[Z(x_i), Z(x_j)] = \sigma^2 R^{'}(x_i, x_j) \qquad (6.8)$$

where σ^2, $R^{'}$ are process variance and correlation which is often expressed as Gaussian [33].

(3) Radial Basis Functions:

The advantage of this model is it has good fits to deterministic and stochastic functions. It can be expressed as a simple kind of neural network, which is established by the distance from the origin. The formulation of RBF can be written as:

$$\hat{y} = \sum_i a_i \,\|\, \mathbf{X} - \mathbf{X}_{0i} \,\| \tag{6.9}$$

where a_i is coefficient, and the norm $\| \mathbf{X} - \mathbf{X}_{0i} \|$ is usually Euclidean distance [33].

6.3.3 Selection and Validation of Surrogate Model

Eleven candidates of surrogate models are constructed based on the 135 training points. In order to confirm the accuracy of surrogate models, the other five testing points are produced using LHS method.

Normalized root mean square error (NRMSE) and R-squared (R^2) are used to determine how well data fit the surrogate model.

(1) Normalized root mean square error:

$$\mathrm{RMSE} = \sqrt{\frac{\sum_{i=1}^{m} (\hat{y}_i - y_i)^2}{m}}$$
$$\mathrm{NRMSE} = \frac{\mathrm{RMSE}}{\hat{y}_{i\max} - \hat{y}_{i\min}} \tag{6.10}$$

where $\hat{y}_i$, y_i, m indicate true value, value of surrogate model, number of test points, respectively.

(2) R-squared:

$$
\begin{aligned}
\bar{y} &= \frac{1}{m}\sum_{i=1}^{m}\hat{y}_i \\
SS_{tot} &= \sum_{i=1}^{m}(\hat{y}_i - \bar{y})^2 \\
SS_{res} &= \sum_{i=1}^{m}(\hat{y}_i - y_i)^2 \\
R^2 &= 1 - \frac{SS_{res}}{SS_{tot}}
\end{aligned}
\tag{6.11}
$$

where $\hat{y}_i$, y_i, $\bar{y}$, m indicate true value, value of surrogate model, mean of true value, and number of test points, respectively.

If NRMSE and R^2 are close to 0 and 1, while the trend of true value and value of surrogate model are similar, the surrogate model is acceptable.

From the comparison among eleven types of surrogate models, simple quadratic of polynomial regression and simple quadratic of Kriging are acceptable to model Maximum Principal Stress of piezoelectric patch and output energy (See Table 9). The trend of two models are very similar as shown in Figure 6-2 and Figure 6-3.

Table 9 Choices of Surrogate Model

	Maximum Principal Stress of Piezoelectric Patch	**Energy**
Model	Polynomial (Simple Quadratic)	Kriging (Simple Quadratic)
NRMSE	1.8 %	6.7 %
R^2	0.9972	0.9615

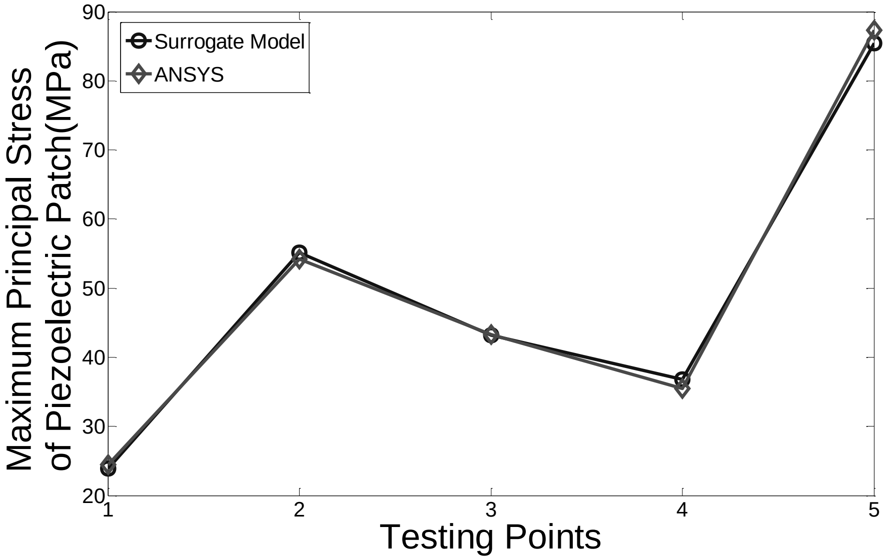

Figure 6-2 Trend of Maximum Principal Stress of Piezoelectric Patch via Testing Points

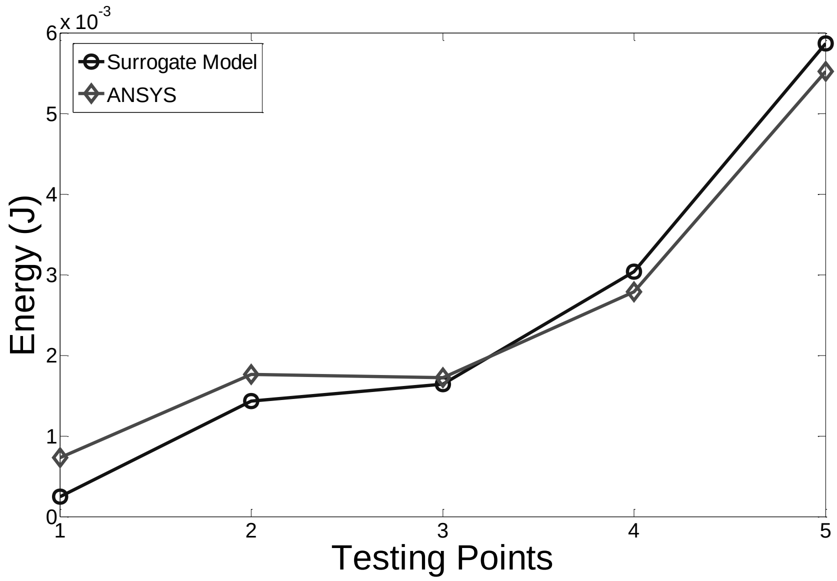

Figure 6-3 Trend of Output Energy via Testing Points

6.4 Results of Design Optimization

The result of design optimization is summarized in Table 10 indicating three merits.

(1) Because RBDO considers the reliability of the structure when attempts to obtain maximum output energy, reliability substantially increases from 65.2% (DO) to 99.58% (RBDO) instead sacrifice of output energy,

(2) Since the thickness of substrate get thicker, Maximum Principal Stress of piezoelectric patch is decreased. At the same time, the delivery of strain to the piezoelectric path become smaller, which results in the decrease of output energy.

(3) On account of numerical error, after RBDO, reliability of OEH sidewalk block

is a little smaller than defined target reliability (99.87%).

Furthermore, the design configurations after DDO and RBDO are shown in Figure 6-4.

Table 10 Design Optimization Result

Category	Notation	DDO		RBDO	
Input Design Variable	r_i **[m]**	27.02		24.63	
	r_o **[m]**	125.44		120.79	
	t **[m]**	3.25		3.73	
	R **[kΩ]**	416.36		476.97	
Output Performance	**E [J]**	0.0138 (Surrogate)	0.0124 (ANSYS)	0.00918 (Surrogate)	0.00894 (ANSYS)
	σ_{PZT} **[MPa]**	48.58 (Surrogate)	45.29 (ANSYS)	39.18 (Surrogate)	37.61 (ANSYS)
Reliability		65.2 %		99.58 %	

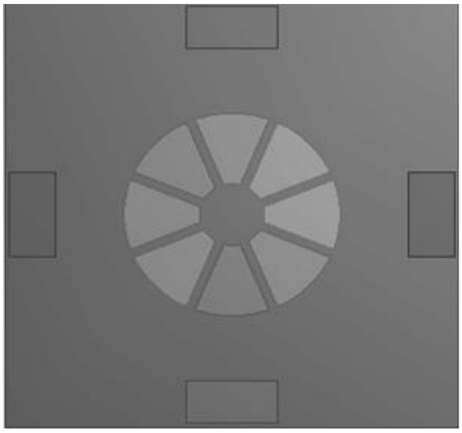

(a)

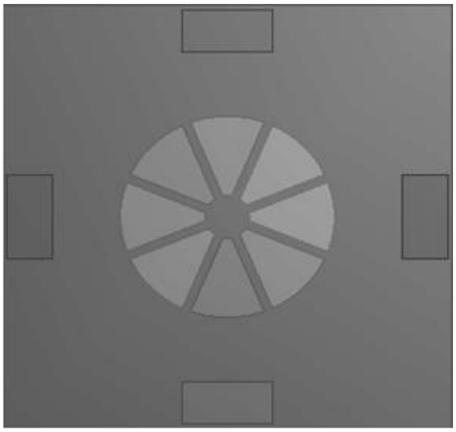

(b)

Figure 6-4 Design Configuration Results (a) DDO and (b) RBDO

Chapter 7. Conclusions and Future Works

7.1 Conclusion

This study aims at developing an omnidirectional energy harvesting sidewalk (OEH) block based on a piezoelectric EH skin concept. Unlike commercially available energy harvesting sidewalk blocks, the proposed OEH sidewalk block is designed as a scientific approach via four steps: (1) normal gait load profile is extracted from human gait analysis, which is used for designing OEH sidewalk block, (2) conceptual design of OEH sidewalk block is developed by considering directional uncertainty of human footstep, (3) multiphysics simulation of OEH sidewalk block is performed to estimate the time-variant piezoelectric behaviors (mechanical stress and output voltage) under transient loading profile of normal gait, and (4) reliability-based design optimization (RBDO) of OEH sidewalk block with surrogate model is implemented to maximize the output energy while considering the variability in normal gait, material properties, and geometry. For the purpose of efficiently performing RBDO, Kriging and polynomial surrogate models were constructed based on the Latin Hypercube sampling (LHS) which is a space filling technique. Furthermore, in RBDO, Progressive Quadratic Response Surface Method (PQRSM) and Monte-Carlo Simulation were conducted for design optimization and reliability analysis, respectively. Finally, the reliability of the proposed OEH sidewalk block was 99.58 % and the corresponding output energy was 0.00914 J.

7.2 Contribution

Based on the above procedure, this study has the following three contributions: (1) systematic design rationales of OEH sidewalk block (2) multiphysics finite element modeling under transient normal gait and (3) reliability-based design optimization with surrogate model with respect to the electromechanical behavior of piezoelectric energy harvesting

Contribution 1: Systematic Design Rationales of OEH Sidewalk Block

Omnidirectional concept for energy harvesting sidewalk block is proposed by considering directional uncertainty of normal gait. In this thesis, furthermore, strain distributions of OEH sidewalk block are used to determine the shape and position of piezoelectric patches based on loading profile extracted from the ground reaction force of normal gait. For the purpose of avoiding voltage cancellation, piezoelectric material segmentation is applied for energy harvesting sidewalk block. In addition, since human walking is an intermittent activity, the output power might be also generated intermittently. However, because the objective function is formulated with respect to not electric power but electric energy under the given time duration in a design process, external capacitor can be used to make an energy storage system for stably charging electrical device or powering transportation equipment.

Contribution 2: Multiphysics Finite Element Modeling under Transient Normal Gait

In this thesis, multiphysics finite element modeling of OEH sidewalk block is developed according to human normal gait. This multiphysics finite element modeling can perform electromechanically-coupled simulation for piezoelectric energy harvesting. Furthermore, ground reaction force during stance phase is implemented to simulate transient loading profile of normal gait. With respect to equivalent circuit model for piezoelectric analysis, time constant of RC circuit under transient loading condition causes electric damping effect, which leads to time-variant voltage and energy. Therefore, unlike the previous research of PEH for the output voltage and/or power maximization, this thesis implemented energy maximization formulation by considering time-variant behavior with respect to change of external electrical resistance.

Contribution 3: Reliability-Based Design Optimization for Piezoelectric Energy Harvesting Using Surrogate Model

In this thesis, RBDO is performed from an electromechanical point of view. For a mechanical response, the mechanical stresses of substrate and piezoelectric patch are compared with fatigue failure constraints to ensure the reliability, while electric energy maximization is implemented as an objective function from the perspective of the electrical domain to enhance the efficiency of OEH sidewalk block. Therefore, an integrated design optimization is successfully executed for designing optimal reliable OEH sidewalk block while considering the variability in geometry and material properties.

7.3 Future Work

Although the OEH sidewalk block is successfully developed in this thesis, it still requires many additional effort to improve the proposed OEH sidewalk block.

(1) Topology Optimization of OEH sidewalk Block

In this thesis, the shape and size of piezoelectric patches of OEH sidewalk block were defined to cover the all positions of sole of the foot. As a future work, topology optimization can be performed in a design process to save the material cost while producing the maximum output energy of OEH sidewalk block.

(2) Optimal Materials Selection

In order to harvest more electric energy from human gait, material selection of OEH sidewalk block can be an important issue. Even though a large amount of deflection can generate more electric energy, however, people may feel uncomfortable when walking on the sidewalk block. Therefore, kinematics design is recommended to solve this practical issue. Furthermore, it might be a good option to use a recyclable green material for the protection of environment.

(3) Electrical Circuit Optimization for Output Energy Regulation

Since human walking motion is a discontinuous activity, the output energy might be also discontinuous, and thus it results in deficiency for the stable use of the output energy. Therefore, to employ electric energy sustainably, an optimal electrical circuit should be established for regulate the output energy.

Bibliography

[1] D. Christin, A. Reinhardt, P. S. Mogre, and R. Steinmetz, "Wireless sensor networks and the internet of things: Selected challenges," *Proceedings of the 8th GI/ITG KuVS Fachgespräch Drahtlose Sensornetze,* pp. 31-34, 2009.

[2] H. Yoon and B. D. Youn, "Stochastic quantification of the electric power generated by a piezoelectric energy harvester using a time–frequency analysis under non-stationary random vibrations," *Smart Materials and Structures,* vol. 23, p. 045035, 2014.

[3] A. Erturk and D. J. Inman, *Piezoelectric energy harvesting*: John Wiley & Sons, 2011.

[4] H. Yoon, "Analytical model for electric power prediction of piezoelectric energy harvesting," Master's Thesis, Department of Mechanical and Aerospace Engineering, Seoul National University, Seoul, 2013.

[5] F. Goldschmidtboeing and P. Woias, "Characterization of different beam shapes for piezoelectric energy harvesting," *Journal of micromechanics and microengineering,* vol. 18, p. 104013, 2008.

[6] S. Lee and B. D. Youn, "A new piezoelectric energy harvesting design concept: multimodal energy harvesting skin," *Ultrasonics, Ferroelectrics, and Frequency Control, IEEE Transactions on,* vol. 58, pp. 629-645, 2011.

[7] C. Dagdeviren, Y. Su, P. Joe, R. Yona, Y. Liu, Y.-S. Kim, *et al.*, "Conformable amplified lead zirconate titanate sensors with enhanced piezoelectric response for cutaneous pressure monitoring," *Nature communications*, vol. 5, 2014.

[8] C. Dagdeviren, B. D. Yang, Y. Su, P. L. Tran, P. Joe, E. Anderson, *et al.*, "Conformal piezoelectric energy harvesting and storage from motions of the heart, lung, and diaphragm," *Proceedings of the National Academy of Sciences*, vol. 111, pp. 1927-1932, 2014.

[9] B. Yang and K.-S. Yun, "Piezoelectric shell structures as wearable energy harvesters for effective power generation at low-frequency movement," *Sensors and Actuators A: Physical*, vol. 188, pp. 427-433, 2012.

[10] N. S. Shenck and J. A. Paradiso, "Energy scavenging with shoe-mounted piezoelectrics," *IEEE micro*, pp. 30-42, 2001.

[11] S. T, "Human powered wearable computing," *IBM Syst J 35(3–4):618–29,* 1996.

[12] P. J. Starner T, "Human generated power for mobile electronics," *In: Piguet G (ed) Low power electronics design. CRC, Boca Raton, FL,* 2004.

[13] P. Niu, P. Chapman, R. Riemer, and X. Zhang, "Evaluation of motions and actuation methods for biomechanical energy harvesting," in *Power Electronics Specialists Conference, 2004. PESC 04. 2004 IEEE 35th Annual*, 2004, pp. 2100-2106.

[14] Pavegen (Online), available from: www.pavegen.com.

[15] F. Duarte, F. Casimiro, D. Correia, R. Mendes, and A. Ferreira, "A new pavement energy harvest system," in *Renewable and Sustainable Energy Conference (IRSEC), 2013 International*, 2013, pp. 408-413.

[16] J. Cramm, A. El-Sherif, J. Lee, and J. Loughlin, "Investigating the feasibility of implementing Pavegen energy: harvesting piezoelectric floor tiles in the new SUB," 2011.

[17] Waynergy (Online), available from: www.waydip.com.

[18] D. H. Sutherland, "The evolution of clinical gait analysis part l: kinesiological EMG," *Gait & posture,* vol. 14, pp. 61-70, 2001.

[19] M. W. Whittle, *Gait analysis: an introduction*: Butterworth-Heinemann, 2014.

[20] T. Keller, A. Weisberger, J. Ray, S. Hasan, R. Shiavi, and D. Spengler, "Relationship between vertical ground reaction force and speed during walking, slow jogging, and running," *Clinical Biomechanics,* vol. 11, pp. 253-259, 1996.

[21] A. E. Hunt, R. M. Smith, M. Torode, and A.-M. Keenan, "Inter-segment foot motion and ground reaction forces over the stance phase of walking," *Clinical Biomechanics,* vol. 16, pp. 592-600, 2001.

[22] S. Lee and B. D. Youn, "A design and experimental verification

methodology for an energy harvester skin structure," *Smart Materials and Structures*, vol. 20, p. 057001, 2011.

[23] T. Stepinski, T. Uhl, and W. Staszewski, *Advanced Structural Damage Detection: From Theory to Engineering Applications*: John Wiley & Sons, 2013.

[24] Engineering Fundamentals Inc. IHS GlobalSpec (Online), available from: www.efunda.com/materials/piezo/material_data/matdata output.cfm?Material ID=PZT5H

[25] T. Ng and W. Liao, "Sensitivity analysis and energy harvesting for a self-powered piezoelectric sensor," *Journal of Intelligent Material Systems and Structures*, vol. 16, pp. 785-797, 2005.

[26] D. Upadrashta, Y. Yang, and L. Tang, "Material strength consideration in the design optimization of nonlinear energy harvester," *Journal of Intelligent Material Systems and Structures*, p. 1045389X14546651, 2014.

[27] C. Hu, B. D. Youn, and H. Yoon, "An adaptive dimension decomposition and reselection method for reliability analysis," *Structural and Multidisciplinary Optimization*, vol. 47, pp. 423-440, 2013.

[28] S. Mahadevan, "Monte carlo simulation," *MECHANICAL ENGINEERING-NEW YORK AND BASEL-MARCEL DEKKER-*, pp. 123-146, 1997.

[29] N. E. Dowling, *Mechanical behavior of materials: engineering methods for*

deformation, fracture, and fatigue: Prentice hall, 1993.

[30] "Structural steel fatigue data at zero mean stress," *ASME BPV Code, Section 8, Div 2, Table 5-110.1,* 1998.

[31] G. G. Wang and S. Shan, "Review of Metamodeling Techniques in Support of Engineering Design Optimization," *Journal of Mechanical Design,* vol. 129, pp. 370-380, 2007.

[32] B. Minasny and A. B. McBratney, "A conditioned Latin hypercube method for sampling in the presence of ancillary information," *Computers & Geosciences,* vol. 32, pp. 1378-1388, 2006.

[33] R. Jin, W. Chen, and T. W. Simpson, "Comparative studies of metamodelling techniques under multiple modelling criteria," *Structural and Multidisciplinary Optimization*, vol. 23, pp. 1-13, 2001.

국문 초록

우리 주변에서 버려지는 역학적 에너지로부터 전기 에너지를 수확하여 각종 무선 센서 및 저전력 소형 전자기기를 구동해서 반영구적으로 사용할 수 있는 압전 에너지 하베스팅 기술이 큰 각광을 받고 있다. 압전 에너지 하베스팅 기술은 압전 소자에 물리적 변형이 인가되면 전기적 편극이 발생하는 압전 효과를 이용하는 것으로, 에너지 밀도가 높고 설치가 용이하다는 장점이 있다.

특히 최근에는 압전 에너지 하베스팅 기술을 적용하여 인체의 다양한 움직임으로부터 전기 에너지를 수확하는 연구들이 많이 수행되고 있다. 그 중에서, 인체 보행 시 지면에 가해지는 하중을 이용하여 전기 에너지를 수확할 수 있는 에너지 하베스팅 보도블록이 상용 제품으로 출시되어 공공장소에 설치해서 사용한바 있다.

하지만 인체 보행 특성이 압전 소자의 전기-기계적 거동에 미치는 영향을 체계적으로 분석하여 에너지 하베스팅 보도블록 개발에 접목한 연구는 보고된 바 없으며, 특히 인체 보행 불규칙성 및 압전 소자 물성 산포 등의 불확실성 하에서 안정적으로 에너지를 수확하면서도 피로 파괴에 의한 내구/신뢰성을 보장할 수 있는 체계적이고 과학적인 설계 방법론은 전무하다.

따라서 본 논문에서는 인체 보행 특성과 압전 에너지 변환의 물리적 메커니즘을 통합적으로 고려한 전방향 에너지 하베스팅 보도블록 설계 방법론을 제안하고자 한다. 본 논문에서 제안된 설계 방법론은 네 가지 단계가 순차적으로 진행된다. 먼저, 인체 보행 분석에 의한 지면 반력 하중으로부터 정상 보행 하중 프로파일을 추출한다. 두 번째 단계에서는

인체 보행 시 걸음 방향의 불규칙성을 고려한 전방향 압전 소자 배치 기술과, 보행 하중에 의하여 보도블록에 인가되는 변형율의 변곡선 부근에서 발생하는 전압 상쇄 현상을 방지할 수 있는 압전 소자 분할 기술 등이 적용된 개념 설계를 제안한다. 세 번째 단계에서는 정상 보행 하중 프로파일 하에서 전방향 에너지 하베스팅 보도블록의 시변 전압 및 응력 변화를 예측하기 위하여, 과도 하중에서 전기-기계 연성 시뮬레이션을 수행할 수 있는 다물리 유한요소모델을 개발한다. 마지막으로 네 번째 단계에서는 인체 보행, 소자 물성, 제작 공차 등에 내포된 불확실성을 고려하여 전방향 에너지 하베스팅 보도블의 최종 설계를 도출할 수 있는 신뢰성 기반 최적설계를 수행한다. 특히 효율적인 신뢰성 기반 최적설계를 위하여 대표적인 공간 충진 기법 중에 하나인 라틴방격 추출법(Latin Hypercube Design)로 전산실험계획을 수행하고, 이를 기반으로 크리깅(Kriging)과 다항식 회귀분석 기법으로 대리모델을 구축하였다.

본 논문에서 제안된 설계 방법론을 통하여 개발된 전방향 에너지 하베스팅 보도블록은 대한민국 성인 남성 평균 체중(70 kg)을 기준으로 약 8.94 mJ의 에너지를 수확할 수 있다. 다음 취성재료인 압전 소자의 피로 강도(48.3 MPa)에 대하여 최대 주응력을 기준으로 계산된 신뢰도는 약 99.58 %였으며, 이 때의 최대 주응력은 약 37.61 MPa였다.

주요어: 압전 에너지 하베스팅
전방향 에너지 하베스팅 보도블록
인체 보행 분석
전압 상쇄 현상
다물리 전기-기계 연성 시뮬레이션
신뢰성 기반 최적설계
대리모델

학 번: 2013-23827